High field Q slope and the effect of low-temperature baking at 3 GHz

G. Ciovati
Thomas Jefferson National Accelerator Facility, Newport News, Virginia 23606, USA and Department of Physics, Center for Accelerator Science, Old Dominion University, Norfolk, Virginia 23529, USA

G. Eremeev and F. Hannon
Thomas Jefferson National Accelerator Facility, Newport News, Virginia 23606, USA

(Received 17 October 2017; published 29 January 2018)

A strong degradation of the unloaded quality factor with field, called high field Q slope, is commonly observed above $B_p \cong 100$ mT in elliptical superconducting niobium cavities at 1.3 and 1.5 GHz. In the present experiments several 3 GHz niobium cavities were measured up to and above $B_p \cong 100$ mT. The measurements show that a high field Q slope phenomenon limits the field reach at this frequency, that the high field Q slope onset field depends weakly on the frequency, and that the high field Q slope can be removed by the typical empirical solution of electropolishing followed by heating to 120°C for 48 hrs. In addition, one of the cavities reached a quench field of 174 mT and its field dependence of the quality factor was compared against global heating predicted by a thermal feedback model.

DOI: 10.1103/PhysRevAccelBeams.21.012002

I. INTRODUCTION

Radio-frequency surface resistance of superconducting niobium exhibits field dependence, which changes drastically with surface treatment and preparation. One of the common field dependencies, typically observed after chemical treatment in 1.3 and 1.5 GHz elliptical cavities, is the so-called *high field Q slope* (HFQS). The high field Q slope was identified in the 1990s [1], when advances with high pressure rinsing allowed for field emission free cavities reaching peak magnetic fields (B_p) above 100 mT. Since the typical ratio of peak magnetic field to accelerating gradient in elliptical cavities is about 4–5 mT/(MV/m), cavities were reaching accelerating gradients (E_{acc}) in excess of 20 MV/m. At this field a strong degradation in the quality factor was consistently observed in 1.3 and 1.5 GHz cavities without any x-ray production. Further experiments with temperature mapping indicated broad heating in the high magnetic field regions [2–4]. In the late 1990s–early 2000s an empirical solution was found to remove the degradation: 120 °C baking for 48 hours [5,6]. The solution resulted in high gradient niobium cavities and is used today as a standard treatment for many projects.

As part of a new material development program, 3 GHz cavities were built out of niobium to serve as a substrate for future new material coatings. The cavities received the standard cavity processing and were measured at the helium bath temperature (T_b) of 2.0 K to confirm their suitability as a substrate. Several cavities reached high fields and were limited by a Q slope reminiscent of the high field Q slope.

There are ample data on this degradation in elliptical cavities at 1.5 and 1.3 GHz, but fewer rf measurements have been done at other frequencies [7–10]. Hence, one of the questions regarding HFQS is its frequency dependence. Since most of the data related to the degradation were collected at 1.3 or 1.5 GHz, models are required to predict the frequency of the onset of the HFQS. This question was addressed in the past using the data sets available at the time [11,12]. Results at 3 GHz reported here suggest that 3 GHz cavities are limited by the same phenomenon that can limit the field reach at lower frequencies. The results also show that accelerating gradients above 30 MV/m, and in one case up to ~41 MV/m, can be reached even at these frequencies with the correct treatment.

The importance of this finding is illustrated, for example, by the fact that the choice of frequency for TESLA cavities was in part driven by what was considered to limit high frequency cavities [13].

II. CAVITY PROCESSING AND TEST RESULTS

Five cavities, designated FH3A, FH3C, FH3D, FH3E, and FH3F were used in these experiments. The cell shape is that of the TESLA long end half cell [13] scaled to 3 GHz, Fig. 1. The main electromagnetic parameters are

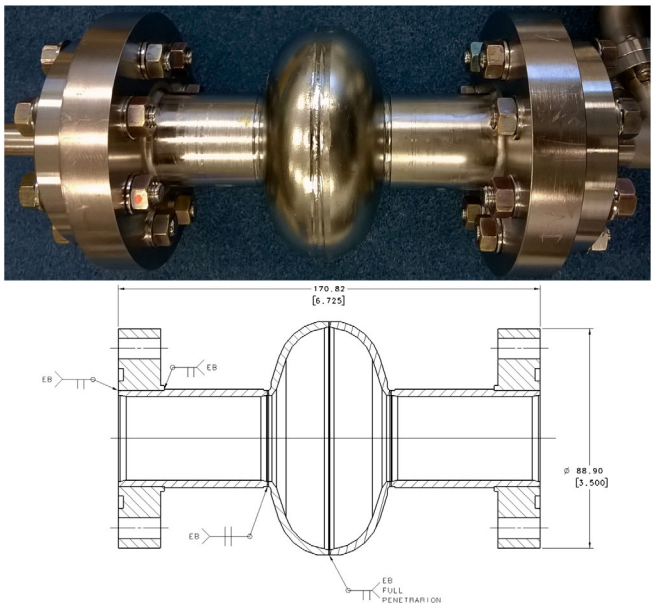

FIG. 1. The photo of FH3A assembled for testing is shown in the top. The sketch of the cavity shape, which is the TESLA long end half cell [13] scaled to 3 GHz, is shown in the bottom. Dimensions are in mm [inches].

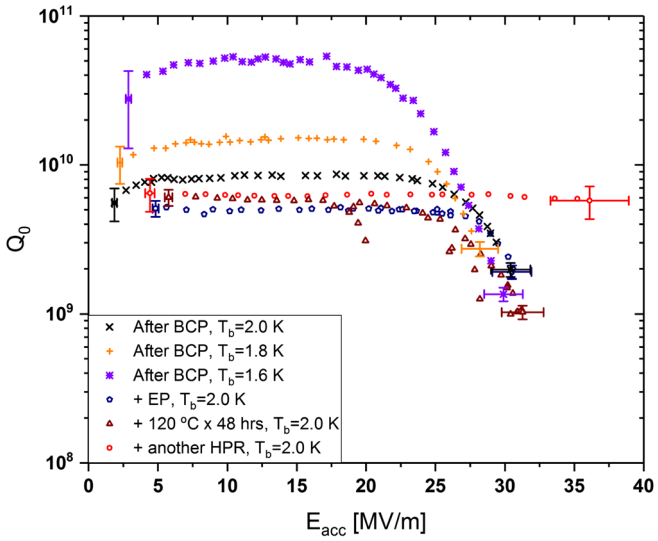

FIG. 2. FH3C test results after BCP treatment for three different helium bath temperatures, 2.0, 1.8, 1.6 K and after EP treatment and mild baking at $T_b = 2.0$ K. Note the increase in the low-field quality factor as expected for lower helium bath temperatures, but similar Q drops. Also, note the absence of the high-field degradation in the test after the EP and mild baking.

$B_p/E_{acc} = 4.23$ mT/(MV/m), $G = 277.9\ \Omega$, which is the geometry factor, and $R/Q = 105\ \Omega$, which is the shunt impedance divided by the quality factor. The half cells were stamped from 3 mm high purity (RRR ~ 300) niobium disks, mechanically polished, and electron beam welded together along with cutoff tubes and flanges to form 3 GHz single-cell cavities. FH3A, FH3C, FH3D, and FH3E were made out high purity fine grain material, and FH3F was made out of high purity large grain material. FH3A, FH3C and FH3D received 80 μm of buffered chemical polishing, BCP (1:1:1). The chemical etching was split into four steps to improve the removal uniformity with cavity being flipped between each treatment. After BCP the cavities were annealed in a vacuum furnace at 600 °C for 10 hours followed by an additional etching with BCP (1:1:1) solution to remove 10 μm. Additional treatments consisting of centrifugal barrel polishing, vacuum annealing at 600 °C for 10 hours and electropolishing (EP) were applied to FH3A to improve its performance. FH3E received 110 μm BCP (1:1:1), was annealed at 800 °C for 2 hours, and etched for an additional 60 μm with BCP (1:1:1). FH3F received 90 μm BCP (1:1:1), was annealed at 800 °C for 3 hours, and etched for an additional 25 μm with BCP (1:1:1). Prior to the cryogenic rf power test, each cavity was high-pressure rinsed with ultrapure water, assembled with rf antennas and vacuum flanges and evacuated to $< 10^{-7}$ mbar.

FH3C was first tested at 2.0 K. The cavity had a low-field quality factor of about 8×10^9 at $T_b = 2.0$ K. Above $E_{acc} = 20$ MV/m a rapid degradation of the quality factor set in. The cavity was limited to E_{acc} of about 30 MV/m, where the quality factor degraded to about 1×10^9, Fig. 2. At this point the test was limited by the 60 Watt available rf input power due to the coupling mismatch of the fixed coupler. With the cavity still in the Dewar, the Dewar was topped off with liquid helium the next day and the cavity was tested at $T_b = 1.8$ K and $T_b = 1.6$ K. The low-field quality factor has improved reaching 1.5×10^{10} at $T_b = 1.8$ K and 5.3×10^{10} at $T_b = 1.6$ K. However, the Q drop was still present and limited the cavity to $E_{acc} \cong 30$ MV/m.

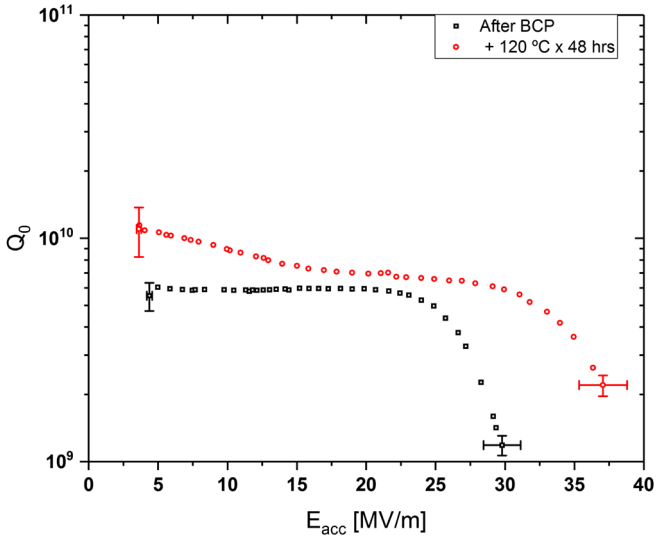

FIG. 3. FH3D test results at $T_b = 2.0$ K before and after baking at 120 °C for 48 hours. No radiation was observed during the measurements.

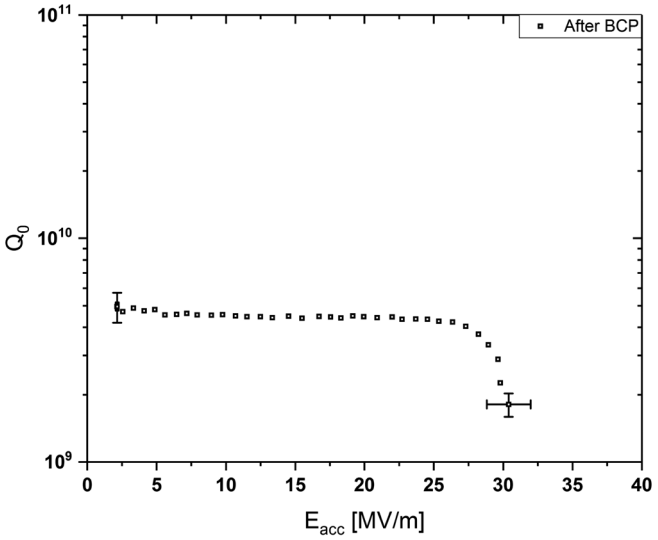

FIG. 4. FH3E test results at $T_b = 2.0$ K. Note the characteristic high-field degradation.

No x-ray radiation was observed during the measurements. After the test FH3C was removed from the Dewar and disassembled. FH3C was then chemically treated again. This time the JLab horizontal electropolishing machine was used. The cavity was electropolished similar to the 12 GeV CEBAF upgrade cavity (C100) electropolishing procedure [14], except a special aluminum cathode was built to accommodate smaller beam tubes. The cavity was electropolished in two steps for a total of 40 μm. After electropolishing FH3C was HPRed, assembled in a cleanroom, evacuated, and tested again at 2.0 K. Q_0 at 2 K was at about 5×10^9 up to about $E_{acc} = 25$ MV/m, where a strong Q drop set in. The intrinsic quality factor dropped to about

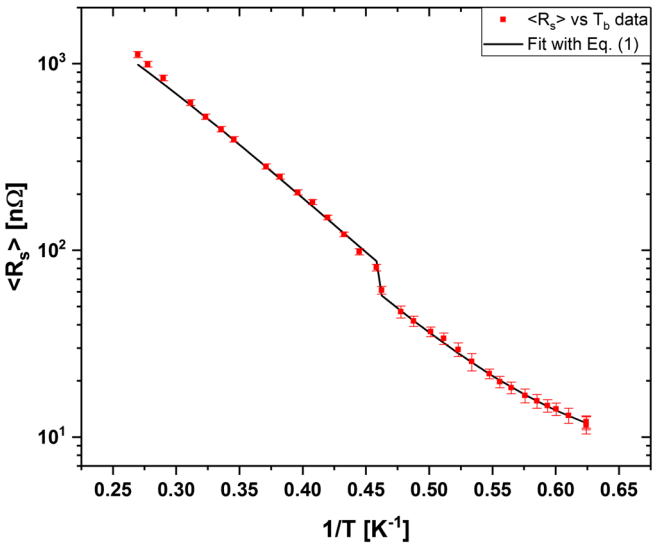

FIG. 5. FH3A data between $T_b = 3.7$ K and $T_b = 1.6$ K at $E_{acc} \sim 4.2$ MV/m. The solid black line was obtained from a least-squares fit with Eq. (1).

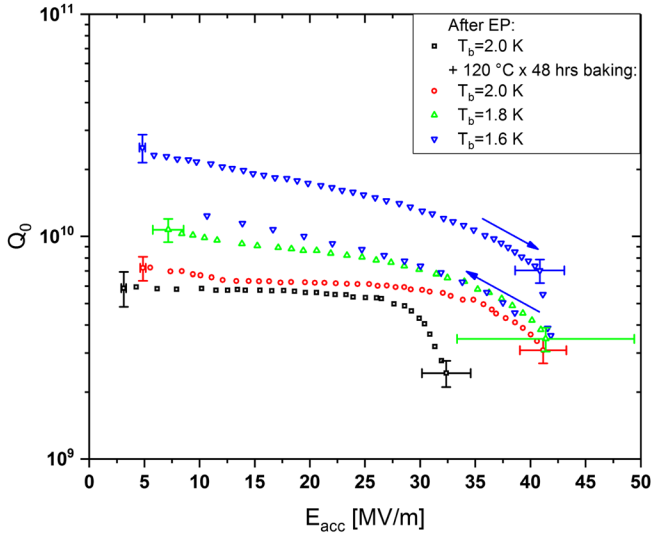

FIG. 6. FH3A test results at $T_b = 2.0$ K and at $T_b = 2.0$ K, $T_b = 1.8$ K, and $T_b = 1.6$ K after 120 °C baking. Note the characteristic high-field degradation before 120 °C baking. Q_0 dropped after multiple quenches at 1.6 K as shown by the data measured while lowering the field after quench, indicated by the arrow.

2×10^9 at $E_{acc} = 30.5$ MV/m, limited by available rf power. No x rays were observed in the test. After the second test, FH3C was removed from the Dewar, baked *in situ* at 120 °C for 48 hours, and tested again at 2.0 K. After baking, the low-field quality factor improved to about 6×10^9 at 2 K. The cavity was still limited to a similar gradient of $E_{acc} = 30$ MV/m by a strong Q drop. However, during this test x rays up to 0.2 mSv/hour at the highest gradient were observed. Finally, the cavity was removed from the Dewar, disassembled, HPRed, assembled in the

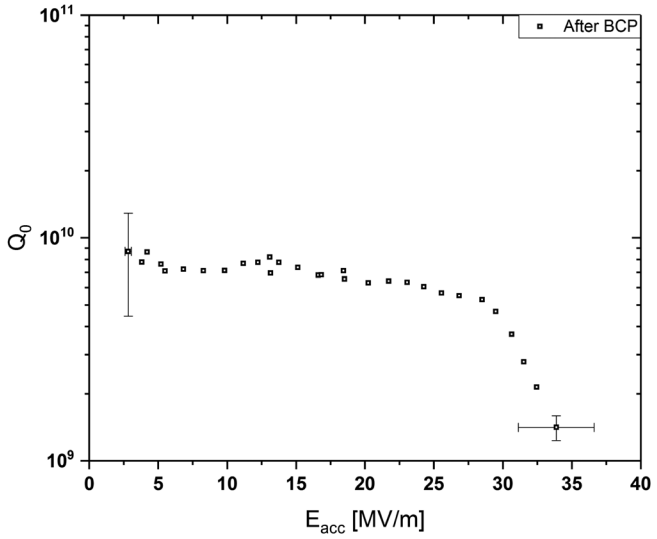

FIG. 7. FH3F test results at $T_b = 2.0$ K. Note the characteristic high-field degradation.

TABLE I. This table summarizes the results from all tests.

ID	Helium bath temperature [K]	Q_0 at $E_{acc} \cong 5$ MV/m	Q_0 at E_{max}	Q slope onset E_{acc} [MV/m]	FE onset E_{acc} [MV/m]	Maximum E_{acc} [MV/m]	Limitation	Latest treatment
FH3C	2.0	$(8.2 \pm 1.3) \times 10^9$	$(2.0 \pm 0.2) \times 10^9$	≈20	···	30.4 ± 1.4	Q slope	80 μm BCP (1:1:1) + 600 °C × 10 hrs + 10 μm BCP (1:1:1)
FH3C	1.8	$(1.3 \pm 0.3) \times 10^{10}$	$(2.7 \pm 0.3) \times 10^9$	≈20	···	28.2 ± 1.3	Q slope	Same
FH3C	1.6	$(4.2 \pm 2.7) \times 10^{10}$	$(1.4 \pm 0.1) \times 10^9$	≈20	···	30.0 ± 1.4	Q slope	Same
FH3C	2.0	$(5.1 \pm 0.6) \times 10^9$	$(2.0 \pm 0.2) \times 10^9$	≈25	···	30.6 ± 1.4	Q slope	+40 μm EP
FH3C	2.0	$(6.0 \pm 0.8) \times 10^9$	$(1.0 \pm 0.1) \times 10^9$	≈20	21	31.3 ± 1.5	Q slope	+120 °C × 48 hrs
FH3C	2.0	$(6.4 \pm 1.6) \times 10^9$	$(5.7 \pm 1.4) \times 10^9$	···	···	36.1 ± 2.8	Quench	+ another HPR
FH3D	2.0	$(6.0 \pm 0.9) \times 10^9$	$(1.2 \pm 0.1) \times 10^9$	≈20	···	29.8 ± 1.3	Q slope	80 μm BCP (1:1:1) + 600 °C × 10 hrs + 10 μm BCP (1:1:1)
FH3D	2.0	$(1.1 \pm 0.2) \times 10^{10}$	$(2.2 \pm 0.2) \times 10^9$	≈25	···	37.1 ± 1.7	Q slope	+ 120 °C × 48 hrs
FH3E	2.0	$(4.8 \pm 0.7) \times 10^9$	$(1.8 \pm 0.2) \times 10^9$	≈27	···	30.4 ± 1.6	Q slope	110 μm BCP (1:1:1) + 800 °C × 2 hrs + 60 μm BCP (1:1:1)
FH3A	2.0	$(5.9 \pm 1.0) \times 10^9$	$(2.4 \pm 0.3) \times 10^9$	≈27	···	32.4 ± 2.2	Q slope	80 μm BCP (1:1:1) + 600 °C × 10 hrs + 10 μm BCP (1:1:1) + CBP + 600 °C × 10 hrs + 30 μm EP
FH3A	2.0	$(7.2 \pm 0.9) \times 10^9$	$(3.1 \pm 0.4) \times 10^9$	···	···	41.2 ± 2.1	Quench	+ 120 °C × 48 hrs
FH3A	1.8	$(1.1 \pm 0.1) \times 10^{10}$	$(3.5 \pm 0.4) \times 10^9$	···	···	41.4 ± 8.0	Quench	Same
FH3A	1.6	$(2.5 \pm 0.4) \times 10^{10}$	$(5.5 \pm 0.7) \times 10^9$	···	···	41.1 ± 2.2	Quench	Same
FH3F	2.0	$(7.6 \pm 3.2) \times 10^9$	$(1.4 \pm 0.2) \times 10^9$	≈28	27	33.9 ± 2.7	Q slope	90 μm BCP (1:1:1) + 800 °C × 3 hrs + 25 μm BCP (1:1:1)

cleanroom, and tested again at 2.0 K. In the rf test at 2 K, the low-field quality factor was again at about 6×10^9. This time, no x rays were observed, and the cavity reached $E_{acc} = 36.1$ MV/m without strong quality factor degradation. The cavity was limited by the repeated quench at the highest field, Fig. 2.

FH3D was first tested at 2.0 K. FH3D had a low-field quality factor of about 6×10^9, which stayed constant with field up to $E_{acc} = 20$ MV/m. Above Q slope onset of $E_{acc} = 20$ MV/m, a strong Q_0 degradation was observed, and the cavity was limited by the available power at $E_{acc} \cong 30$ MV/m, Fig. 3. FH3D was then removed from the vertical testing Dewar, baked *in situ* at 120 °C for 48 hours. The cavity was then put back in the Dewar, tested at 2.0 K, and then tested again at 2.0 K two days later. The low-field quality factor improved to about 1×10^{10}, but degraded with field to about 7×10^9 at $E_{acc} = 20$ MV/m. The cavity was limited by a high field Q slope to about $E_{acc} = 37$ MV/m, Fig. 3. No radiation was observed during the measurements.

FH3E was tested at 2.0 K. The cavity had a low-field quality factor of about 5×10^9 at $T_b = 2.0$ K. Above $E_{acc} = 27$ MV/m a rapid degradation of the quality factor set in. The cavity was limited to E_{acc} of about 30 MV/m, where the quality factor degraded to about 2×10^9, Fig. 4. The test was limited by the available rf power. No x rays were observed in the test.

FH3A was tested at 2.0 K. The quality factor at low field was $\sim 6 \times 10^9$ which stayed nearly constant up to $E_{acc} \sim 27$ MV/m above which Q slope set in and Q_0 degraded nearly a factor of 3 at 32.5 MV/m. No x rays were observed in the test. The cavity was baked at 120 °C for 48 hours and retested at 2.0 and 1.8 K. The quality factor at low field at 2 K was $\sim 7 \times 10^9$ and the cavity quenched at 41 MV/m. No x rays were observed in the test. After quenching at 2 K, the surface resistance increased by about 5 nΩ due to trapped magnetic flux. The cavity was warmed up to room temperature to release the trapped flux and cooled back down to 1.6 K. The quality factor at ∼4.2 MV/m was measured as a function of the helium bath temperature between 3.7 and 1.6 K, which was then used to calculate the average surface resistance using $\langle R_s \rangle = G/Q_0$, where G is the geometry factor of the cavity, Fig. 5. The $R_s(T)$ data were used to calculate Q_0 (T, B_p) using the thermal feedback model as discussed in Sec. III. At 1.6 K, $Q_0(E_{acc})$ was measured,

Fig. 6. A few quenches occurred from $E_{acc} \sim 41$ MV/m, causing an increase in the surface resistance by about 10 nΩ, probably, due to the trapped magnetic flux and Q_0 drop to 3.6×10^9 at 41.9 MV/m where repetitive quenches were observed. No x rays were detected in this test. The curves $Q_0(E_{acc})$ before and after baking are shown in Fig. 6.

FH3F was tested at 2.0 K. The quality factor at low field was $\sim 7 \times 10^9$ which stayed nearly constant up to $E_{acc} \sim 28$ MV/m above which Q_0 degraded more than a factor of 3 at 33.9 MV/m, as shown in Fig. 7. X rays corresponding to a dose rate up to ~0.001 mSv/hour were observed in the test above $E_{acc} \sim 27$ MV/m. The test results from all tests are summarized in Table I.

III. DISCUSSION

The quality factor field dependencies observed in all five cavities after EP or BCP have many characteristics of the high field Q slope commonly observed in 1.3 and 1.5 GHz SRF cavities. The high field Q slope is commonly referred to as the degradation of the quality factor at accelerating gradients above 20 MV/m without x rays. While no x rays were observed in the first experiments with the cavities (Figs. 2–4), it may be argued that it was the case due to the smaller accelerating gap of these cavities, of just 5 cm, hence, the same field emission sites may not induce enough radiation to be detected with the standard instrumentation. One possible check in this case would be to test the cavity with a thermometry setup, but such capability was not available at the time. However, the consistency of the observed Q degradations at high field in all four cavities would be surprising to be caused by such a random effect as field emission. Additional indirect evidence, which excludes x rays as the cause for the observed degradation, is the test of FH3C after EP and bake, Fig. 2. After some processing, the cavity was limited by a similar Q slope, but in this test x-ray radiation was observed and was correlated to the quality factor degradation. This supports the viewpoint that x rays will be detected if the heating from field emitted electrons is contributing to the quality factor degradation at the gradients of interest, even in these smaller cavities. Furthermore, in Fig. 8 earlier data on a 3 GHz cavity reproduced from [15] is shown along with our results. The Q slope in the older data has been reported to be common and the thermometry results on those cavities showed broad areas of heating, which indicates that a field emitter was not the limiting cause in those test. The field emission also does not improve after the mild baking [16], which was the case with FH3D, Fig. 3, or FH3A, Fig. 6. Hence, we conclude that the slope in our cavities was not caused by field emission.

In Fig. 9, the rf results after mild baking applied to the BCPed and to the EPed cavity are compared at this frequency. Similar to what has been observed at lower frequencies, mild baking completely eliminates the high field Q slope in the EPed cavity, but does not completely remove it in the fine-grain BCPed cavity. There is a significant improvement in the BCPed cavity after mild baking, but some Q drop persists at high fields. The cavity FH3A quenched at a remarkable peak surface magnetic field of ~180 mT after baking and the Q vs field curves show a mild Q degradation above ~35 MV/m (148 mT).

Thermal feedback can be suggested as the cause of degradation. In the older measurements, reproduced in Fig. 8, the helium bath temperature was not constant during

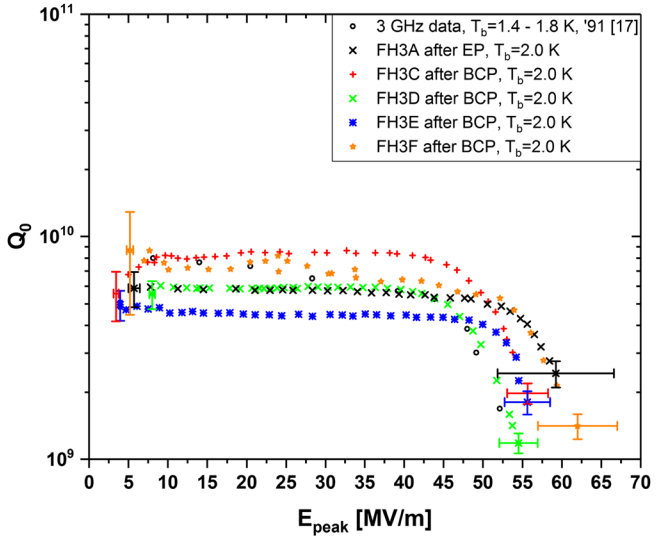

FIG. 8. FH3C, FH3D, and FH3E at $T_b = 2.0$ K are plotted here along with the earlier data reproduced from [15]. $E_{peak}/E_{acc} = 1.83$ was used for the 3 GHz cavities. Note that the temperature of the helium bath increased from about 1.4 K to about 1.8 K with rf dissipated power during the earlier measurements in 1991.

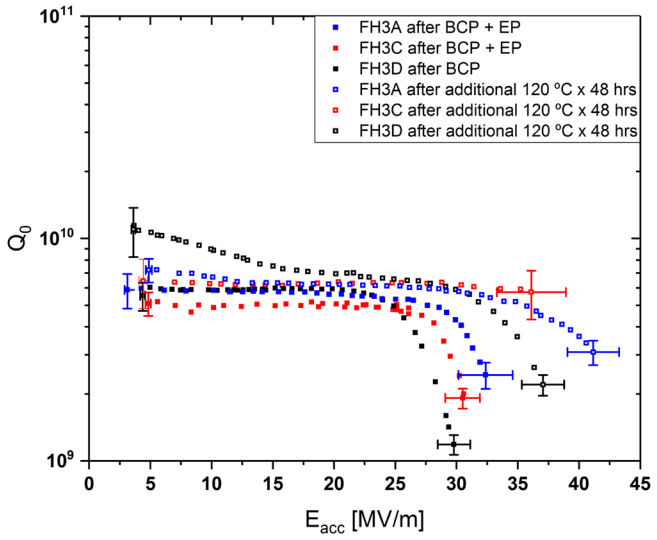

FIG. 9. FH3A, FH3C, and FH3D results before and after mild baking are plotted here. All data is measured at $T_b = 2.0$ K. No field emission was observed in any test.

the rf test, so the Q degradation at high field could be due to increasing He bath temperature [15]. During rf measurements of the cavities reported in this paper, the He bath temperature was kept constant, within $\cong 10$ mK. The rf test of FH3C at three different bath temperatures shows that the slope is not sensitive to such bath temperature variation.

The Q vs field curves measured for cavity FH3A after baking have been analyzed with a thermal feedback model as described in what follows. The surface resistance as a function of the temperature of the inner surface, $R_s(T_s)$, consists of the sum of an analytic expression derived from the Bardeen-Cooper-Schrieffer theory valid in the dirty limit and $T \ll T_c$ [17] and the so-called residual resistance, R_i:

$$R_s(T_s) = \frac{A}{T_s}\ln\left(\frac{2.246 k_B T_s}{hf}\right) e^{-\frac{\Delta}{k_B T_s}} + R_i, \qquad (1)$$

where k_B is the Boltzmann's constant, h is Planck's constant, f is the resonant frequency and Δ is the energy gap. A is a factor that depends on material parameters and it is proportional to f^2. The parameters A, Δ and R_i were obtained by fitting Eq. (1) to the $R_s(T_b)$ data, Fig. 5, using the self-consistent method described in [18] to determine the temperature of the inner surface. The values of the fit parameters are $A = 4.5 \times 10^{-5}\ \Omega\,\mathrm{K}$, $\Delta = 1.36$ meV and $R_i = 7.1\ \mathrm{n}\Omega$. The temperature of the inner surface is calculated as a function of the peak surface magnetic field by solving the one-dimensional heat balance equation [19],

$$\frac{1}{2} R_s(T_s) {H_p}^2 = \frac{T_s - T_b}{R_B(T_b)}, \qquad (2)$$

where $R_B(T_b)$ is the thermal boundary resistance and $H_p = B_p/\mu_0$. $Q_0(B_p)$ can then be estimated as

$$Q_0(B_p) = \frac{G}{R_s[T_s(B_p)]}. \qquad (3)$$

Equation (2) has a real-valued solution only up to a maximum H_p value, H_b, which corresponds to the condition of thermal instability or quench. The values of R_B were chosen such that H_b is equal to the measured quench field for each bath temperature and they were 11, 6 and 4.1 cm^2 K/W at 1.6, 1.8 and 2.0 K, respectively. Such values of R_B are consistent with those recently measured in 1.3 GHz cavities [20]. The $Q_0(B_p)$ curves calculated with the thermal feedback model are shown in Fig. 10 along with the experimental data. The results from the calculation agree qualitatively with the data at 2.0 and 1.8 K and suggest that the Q reduction at high field could be related to a global thermal instability. The model does not reproduce the Q slope measured at 1.6 K and the reason for this is unclear and might be related to an intrinsic nonlinearity of the surface resistance becoming more pronounced at lower temperatures.

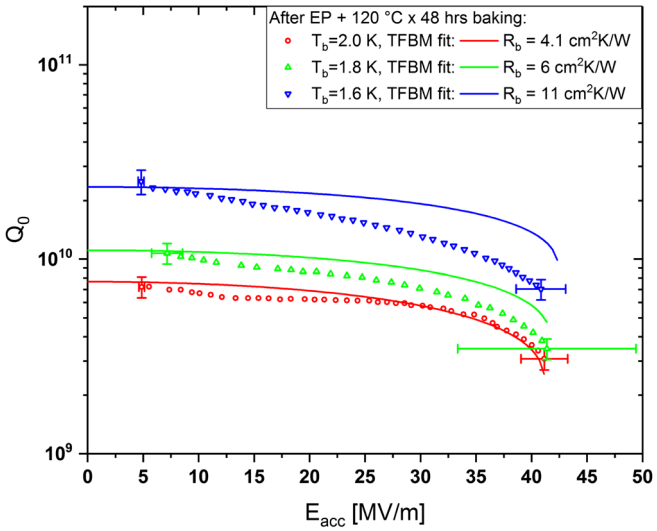

FIG. 10. FH3A test results for three different helium bath temperatures, 2.0, 1.8, 1.6 K (symbols) along with results from a thermal feedback model calculation for each temperature with values of the thermal boundary resistance matching the experimental quench fields (solid lines).

In Fig. 11, we plot our results along with two results for 1.3 and 1.5 GHz single-cell cavities for comparison. In this plot we show a 1.5 GHz one-cell cavity C3C4, which received 20 μm BCP (1:1:2) as the final treatment and a 1.3 GHz one-cell cavity TE1G001, which received 25 μm EP as the final treatment. No x rays were detected in any of the tests. The low-field quality factor of the lower

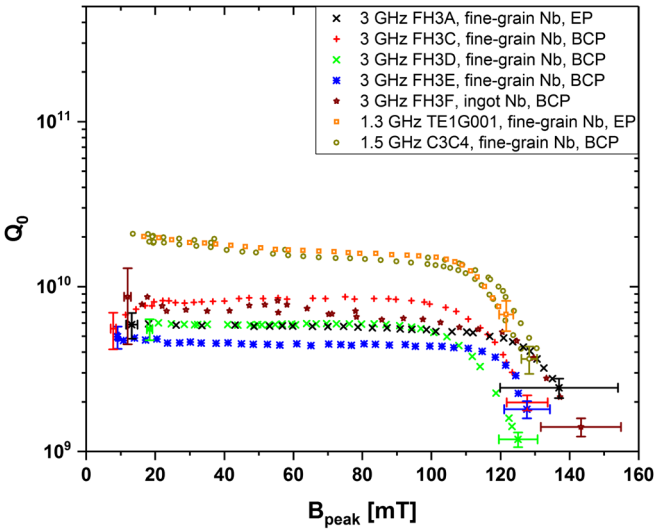

FIG. 11. 3 GHz cavities test results after EP or BCP along with test results for 1.3 GHz and 1.5 GHz single-cell cavities. $B_p/E_{acc} = 4.2$ mT/(MV/m) was used for 1.3 GHz (TESLA end cell); $B_p/E_{acc} = 4.5$ mT/(MV/m) was used for 1.5 GHz [old Cornell (OC) center cell]. All data is measured at $T_b = 2.0$ K. No field emission was observed in any test.

frequency cavities is higher, as expected from the frequency dependence of the BCS part of the surface resistance. At high fields all cavities are limited to about $B_p = 120$–130 mT, and the onset of the high field Q slope is qualitatively quite similar. Onset values for the high field Q slope ranging between 80–125 mT in 1.3–1.5 GHz cavities have been reported in the literature [21,22].

IV. CONCLUSION

The unloaded quality factors of five 3 GHz niobium cavities after various treatments were measured at cryogenic temperatures. A characteristic degradation, the high field Q slope, was observed in all cavities at high fields. The onset of the high field Q slope in the tested 3 GHz cavities was close to 100 mT. The standard solution of electropolishing followed by heating to 120 °C for 48 hours eliminated the high field Q slope in two of the cavities, with one of them reaching 174 mT at 2.0 K. Such a quench field is consistent with the possibility of reaching a global thermal instability as predicted by the standard thermal feedback model.

ACKNOWLEDGMENTS

We would like to thank Jefferson Lab technical staff for technical assistance with surface preparation of the cavities. We would like to thank Pashupati Dhakal for measuring FH3C after electropolishing and baking. This manuscript has been authored by Jefferson Science Associates, LLC under U.S. DOE Contract No. DE-AC05-06OR23177.

[1] B. Bonin and M. Juillard, Progress in RF superconductivity at saclay, in *Proceedings of the 4th European Particle Accelerator Conference, London, England* (EPS-AG, London, 1994), pp. 2045–2047.
[2] L. Lilje, Ph.D. dissertation, Universitaet Hamburg, 2001.
[3] G. Eremeev, Ph.D. dissertation, Cornell University, 2008.
[4] G. Ciovati, Ph.D. dissertation, Old Dominion University, 2005.
[5] J. P. Charrier, B. Coadou, and B. Visentin, Improvements of superconducting cavity performances at high accelerating gradients, in *Proceedings of the 6th European Particle Accelerator Conference, Stockholm, 1998* (IOP, London, 1998), pp. 1885–1887.
[6] K. Saito, H. Inoue, E. Kako, T. Fujino, S. Noguchi, M. Ono, and T. Shishido, Superiority of Electropolishing over Chemical Polishing on High Gradients, in *Proceedings of 8th Workshop on RF Superconductivity, Padova, Italy* (1997), Vol.4, pp. 795–813.
[7] B. Visentin, Low, Medium, High Field Q-Slopes Change with Surface Treatments, in *Proceedings on pushing the limits of rf superconductivity workshop, Argonne, ANL-05/10* (2005), p. 94.
[8] G. Ciovati, P. Kneisel, G. R. Myneni, and S. Chattopadhyay, in *Proceedings of the 23rd International Linac Conference, LINAC-2006, Knoxville, TN, 2006* (JACoW, Knoxville, TN, 2006), p. 318.
[9] G. Ciovati and P. Kneisel, Measurement of the high-field Q drop in the TM010 and TE011 modes in a niobium cavity, Phys. Rev. ST Accel. Beams **9**, 042001 (2006).
[10] P. Pierini *et al.*, Fabrication and vertical test experience of the European X-ray Free Electron Laser 3.9 GHz superconducting cavities, Phys. Rev. Accel. Beams **20**, 042006 (2017).
[11] P. Bauer, G. Ciovati, H. Edwards, J. Halbritter, H. Padamsee, K. Saito, and B. Visentin, A Review of the Q-Drop Phenomenon in High Gradient SRF Cavities, Fermilab technical note, 2006, TD-05-56.
[12] H. Weingarten, Field-dependent surface resistance for superconducting niobium accelerating cavities, Phys. Rev. ST Accel. Beams **14**, 101002 (2011).
[13] B. Aune *et al.*, Superconducting TESLA cavities, Phys. Rev. ST Accel. Beams **3**, 092001 (2000).
[14] A. Reilly, T. Bass, A. Burrill, K. Davis, F. Marhauser, C. E. Reece, and M. Stirbet, Preparation and Testing of the SRF Cavities for the CEBAF 12 GeV Upgrade, in *Proceedings of the 15th International Conference on RF Superconductivity, Chicago, IL, U.S.A.* (2011), pp. 542–548.
[15] H. Padamsee, J. Knobloch, and T. Hays, *RF Superconductivity for Accelerators* (Wiley, New York, 2008).
[16] A. Navitski, S. Lagotzky, D. Reschke, X. Singer, and G. Mueller, Field emitter activation on cleaned crystalline niobium surfaces relevant for superconducting rf technology, Phys. Rev. ST Accel. Beams **16**, 112001 (2013).
[17] A. Gurevich, Superconducting Radio-Frequency Fundamentals for Particle Accelerators, Rev. Accel. Sci. Techol. **05**, 119 (2012).
[18] G. Ciovati, P. Dhakal, and A. Gurevich, Decrease of the surface resistance in superconducting niobium resonator cavities by the microwave field, Appl. Phys. Lett. **104**, 092601 (2014).
[19] A. Gurevich, Multiscale mechanisms of SRF breakdown, Physica C (Amsterdam) **441C**, 38 (2006).
[20] P. Dhakal, G. Ciovati, and G. R. Myneni, Role of Thermal Resistance on the Performance of Superconducting Radio Frequency Cavities, Phys. Rev. Accel. Beams **20**, 032003 (2017).
[21] G. Ciovati, Review of the frontier workshop and Q-slope results, Physica C (Amsterdam) **441C**, 44 (2006).
[22] B. Visentin, Q-slope at high gradients: review of experiments and theories, in *Proceedings of the 11th International Conference on RF Superconductivity, Travemunde, Germany* (2003), p. 199.